



**University of
Zurich**^{UZH}

**Zurich Open Repository and
Archive**

University of Zurich
University Library
Strickhofstrasse 39
CH-8057 Zurich
www.zora.uzh.ch

Year: 2009

Mechanisms of pH-gradient driven transport mediated by organic anion polypeptide transporters

Leuthold, S ; Hagenbuch, B ; Mohebbi, N ; Wagner, C A ; Meier, P J ; Stieger, B

Abstract: Organic anion transporting polypeptides (humans OATPs, rodents Oatps) are expressed in most mammalian tissues and mediate cellular uptake of a wide variety of amphipathic organic compounds such as bile salts, steroid conjugates, oligopeptides, and a large list of drugs, probably by acting as anion exchangers. In the present study we aimed to investigate the role of the extracellular pH on the transport activity of nine human and four rat OATPs/Oatps. Furthermore, we aimed to test the concept that OATP/Oatp transport activity is accompanied by extrusion of bicarbonate. By using amphibian *Xenopus laevis* oocytes expressing OATPs/Oatps and mammalian cell lines stably transfected with OATPs/Oatps, we could demonstrate that in all OATPs/Oatps investigated, with the exception of OATP1C1, a low extracellular pH stimulated transport activity. This stimulation was accompanied by an increased substrate affinity as evidenced by lower apparent Michaelis-Menten constant values. OATP1C1 is lacking a highly conserved histidine in the third transmembrane domain, which was shown by site-directed mutagenesis to be critically involved in the pH dependency of OATPs/Oatps. Using online intracellular pH measurements in OATP/Oatp-transfected Chinese Hamster Ovary (CHO)-K1 cells, we could demonstrate the presence of a 4,4'-diisothiocyanatostilbene-2,2'-disulfonic acid-sensitive chloride/bicarbonate exchanger in CHO-K1 cells and that OATP/Oatp-mediated substrate transport is paralleled by bicarbonate efflux. We conclude that the pH dependency of OATPs/Oatps may lead to a stimulation of substrate transport in an acidic microenvironment and that the OATP/Oatp-mediated substrate transport into cells is generally compensated or accompanied by bicarbonate efflux.

DOI: <https://doi.org/10.1152/ajpcell.00436.2008>

Posted at the Zurich Open Repository and Archive, University of Zurich
ZORA URL: <https://doi.org/10.5167/uzh-17581>
Journal Article

Originally published at:

Leuthold, S; Hagenbuch, B; Mohebbi, N; Wagner, C A; Meier, P J; Stieger, B (2009). Mechanisms of pH-gradient driven transport mediated by organic anion polypeptide transporters. *American Journal of Physiology. Cell Physiology*, 296(3):C570-C582.
DOI: <https://doi.org/10.1152/ajpcell.00436.2008>

Mechanisms of pH-gradient driven transport mediated by organic anion polypeptide transporters

Simone Leuthold,¹ Bruno Hagenbuch,¹ Nilufar Mohebbi,^{2,3} Carsten A. Wagner,^{2,3} Peter J. Meier,¹ and Bruno Stieger^{1,3}

¹Division of Clinical Pharmacology and Toxicology, Department of Medicine, University Hospital; ²Institute of Physiology, University of Zurich; and ³Center for Integrative Human Physiology, University of Zurich, 8057 Zurich, Switzerland

Submitted 24 August 2008; accepted in final form 6 January 2009

Leuthold S, Hagenbuch B, Mohebbi N, Wagner CA, Meier PJ, Stieger B. Mechanisms of pH-gradient driven transport mediated by organic anion polypeptide transporters. *Am J Physiol Cell Physiol* 296: C570–C582, 2009. First published January 6, 2009; doi:10.1152/ajpcell.00436.2008.—Organic anion transporting polypeptides (humans OATPs, rodents Oatps) are expressed in most mammalian tissues and mediate cellular uptake of a wide variety of amphipathic organic compounds such as bile salts, steroid conjugates, oligopeptides, and a large list of drugs, probably by acting as anion exchangers. In the present study we aimed to investigate the role of the extracellular pH on the transport activity of nine human and four rat OATPs/Oatps. Furthermore, we aimed to test the concept that OATP/Oatp transport activity is accompanied by extrusion of bicarbonate. By using amphibian *Xenopus laevis* oocytes expressing OATPs/Oatps and mammalian cell lines stably transfected with OATPs/Oatps, we could demonstrate that in all OATPs/Oatps investigated, with the exception of OATP1C1, a low extracellular pH stimulated transport activity. This stimulation was accompanied by an increased substrate affinity as evidenced by lower apparent Michaelis-Menten constant values. OATP1C1 is lacking a highly conserved histidine in the third transmembrane domain, which was shown by site-directed mutagenesis to be critically involved in the pH dependency of OATPs/Oatps. Using online intracellular pH measurements in OATP/Oatp-transfected Chinese Hamster Ovary (CHO)-K1 cells, we could demonstrate the presence of a 4,4'-diisothiocyanatostilbene-2,2'-disulfonic acid-sensitive chloride/bicarbonate exchanger in CHO-K1 cells and that OATP/Oatp-mediated substrate transport is paralleled by bicarbonate efflux. We conclude that the pH dependency of OATPs/Oatps may lead to a stimulation of substrate transport in an acidic microenvironment and that the OATP/Oatp-mediated substrate transport into cells is generally compensated or accompanied by bicarbonate efflux.

anion/bicarbonate exchange

ORGANIC ANION TRANSPORTING polypeptides (rodents: Oatps; humans: OATPs) constitute a superfamily of sodium-independent membrane transporters belonging to the solute carrier organic anion transporter gene family *Slco/SLCO* (14). All Oatps/OATPs are putative 12 transmembrane domain glycoproteins with apparent molecular masses between 70 to 90 kDa and are generally expressed in multiple organs. However, some OATPs/Oatps are preferentially, if not exclusively, expressed in the liver (e.g., rat Oatp1b2, OATP1B1, OATP1B3), where they are expressed at the basolateral plasma membrane of hepatocytes (5, 24, 25). In hepatocytes, they mediate uptake of amphipathic albumin-bound compounds that are destined for biotransformation and/or biliary excretion (14, 24). Others are

expressed in the brain [OATP1C1, OATP3A1_v1 and v2 (17, 44)] or more specifically in the blood-brain barrier [Oatp1a4 and OATP1A2 (10, 11)]. Functionally, Oatps/OATPs transport in a sodium-independent manner a wide variety of amphipathic organic compounds, including bile salts, steroid conjugates, thyroid hormones, certain oligopeptides, and numerous drugs (14, 26). So far, detailed knowledge on the transport mechanism of OATPs/Oatps is missing, but evidence for a role of bicarbonate as counterion and/or for pH-sensitive uptake with transport stimulation by lower extracellular pH compared with intracellular pH has been presented for rat Oatp1a1 and Oatp1b2 (35, 54) as well as OATP2B1 (23), suggesting an organic anion/OH[−] (or HCO₃[−]) exchange mechanism. Alternatively, substrate exchange for glutathione was demonstrated for Oatp1a1 (32) and glutathione or glutathione conjugates for rat Oatp1a4 (33). Hence, whereas the exact transport mechanism for OATPs/Oatps remains elusive, the current evidence suggests that they act as organic anion exchangers.

In the present study, we tested the hypothesis that stimulation of the transport activity of OATPs/Oatps by a low extracellular pH is a general phenomenon and that this stimulation of transport may be followed by an increase of OATP/Oatp-mediated bicarbonate efflux. We observed that with the exception of OATP1C1, all tested OATPs/Oatps displayed an increased transport activity at an inwardly directed pH gradient in both *Xenopus laevis* oocytes and mammalian cell lines stably transfected with OATPs/Oatps. Site-directed mutagenesis demonstrated that the absence of a highly conserved His in the third transmembrane domain of OATP1C1 was responsible for the lack of pH sensitivity of OATP1C1. Finally, we could demonstrate for selected OATPs/Oatps, substrate transport mediated bicarbonate efflux from stably transfected Chinese Hamster Ovary (CHO)-K1 cells.

MATERIALS AND METHODS

Materials. [³H(G)]taurocholate (TC, 1.19 Ci/mmol, 3.5 Ci/mmol), [6,7-³H(N)]estrone-3-sulfate (E3S, 57.3 Ci/mmol), [5,6,8,11,12,14,15-³H(N)]prostaglandin E₂ (PGE₂, 200 Ci/mmol), and L-[¹²⁵I]thyroxine (T₄, 969 Ci/mmol) were purchased from Perkin-Elmer Life Sciences (Boston, MA). [2-³H]TC (50 Ci/mmol) was additionally obtained from American Radiolabeled Chemicals (St. Louis, MO). Cell culture media and reagents were obtained from Invitrogen (Carlsbad, CA). 4,4'-Diisothiocyanatostilbene-2,2'-disulfonic acid disodium salt (DIDS) was purchased from Sigma (St. Louis, MO). All other chemicals and reagents were of analytical grade and were readily available from commercial sources.

Address for reprint requests and other correspondence: B. Stieger, Univ. Hospital, Dept. of Medicine, Division of Clinical Pharmacology and Toxicology, 8091 Zurich, Switzerland (E-mail: bstieger@kpt.unizh.ch).

The costs of publication of this article were defrayed in part by the payment of page charges. The article must therefore be hereby marked "advertisement" in accordance with 18 U.S.C. Section 1734 solely to indicate this fact.

Animals. Female *X. laevis* were purchased from the African Xenopus facility, Noordhoek, R. South Africa. The animals were kept under standard conditions in accordance with the rules of the local animal protection committee and with the federal guidelines, and the protocols of the animal experiments were approved by the local supervisory board on animal experimentation.

Subcloning of rat *Oatp1b2* and *OATP1B3*. To isolate the rat *Oatp1b2* open reading frame (ORF), the original construct (4) was cut with *SalI* and *HindIII*. The DNA fragment was blunted using T₄ DNA polymerase (Fermentas, St. Leon-Rot, Germany), and the *Oatp1b2* ORF was gel purified from a 0.8% agarose gel using the QIAquick Gel Extraction kit (QIAGEN, Hilden, Germany). The pcDNA5/FRT vector (Invitrogen, Carlsbad, CA) was linearized with *EcoRV*, dephosphorylated with calf intestine alkaline phosphatase (CIAP, Fermentas), and purified with QIAquick PCR purification kit (QIAGEN). The isolated insert was ligated into the pcDNA5/FRT vector using the Rapid DNA Ligation Kit (Roche Diagnostics, Mannheim, Germany). The orientation and DNA sequence of the construct was verified by sequencing.

The cDNA of *OATP1B3* (31) was used to PCR amplify the *OATP1B3* open reading frame (ORF) by Pfu-polymerase (Stratagene, La Jolla, CA) using the forward primer 5'-ACGTACGCTAGCCAC-CATGGACCAACATCAACATTG-3' and the reverse primer 5'-CATGCAGCGGCCGCTTAGTTGGCAGCAGCATTG-3'. The forward primer included a *NheI* restriction site and the Kozak consensus sequence (28) for optimal expression. The reverse primer contained a *NotI* restriction site. The PCR amplified and restriction digested fragment was gel purified and ligated with the Rapid DNA Ligation Kit into the *NheI/NotI* sites of the gel purified, linearized pIRESneo2 vector (Clontech-Takara Bio Europe, Saint-Germain-en-Laye, France). The sequence of the whole ORF was confirmed by DNA sequencing.

Site-directed mutagenesis of *Oatp1a1* and *OATP1C1*. The ORFs of *Oatp1a1* and *OATP1C1* were isolated from pIRESneo2-*Oatp1a1* and pIRESneo2-*OATP1C1* constructs (44) by digestion with *NheI* and *NotI*. After gel purification, the inserts were ligated into the *NheI/NotI* sites of the dephosphorylated pcDNA5/FRT vector. For mutagenesis of the *Oatp1a1* His107 and *OATP1C1* Gln130, point mutations (*Oatp1a1* H107Q and *OATP1C1* Q130H) were introduced using the Quik-Change Mutagenesis XLII Kit (Stratagene, La Jolla, CA). The *NheI/NotI* fragments of the two mutagenized constructs were then again ligated into the *NheI/NotI* sites of dephosphorylated pcDNA5/FRT vector. The sequences of the whole ORF and the presence of the point mutations were confirmed by DNA sequencing.

cRNA synthesis and expression in *X. laevis* oocytes. *Oatp1a1*, *Oatp1a4*, *Oatp1a5*, *Oatp1b2*, *OATP1A2*, *OATP1B1*, *OATP1B3*, *OATP1C1*, *OATP2B1*, *OATP3A1_v1*, *OATP3A1_v2*, *OATP4A1*, and *OATP4C1* cDNAs were available in our laboratory (4, 19, 30, 31, 40, 44). pCMV6-XL4 plasmid (Origene, Rockville, MD) containing either *OATP1B1*, *OATP1B3*, *OATP2B1*, *OATP4A1*, or *OATP4C1* cDNA was linearized with *XbaI*; pSPORT1 plasmid (Invitrogen, Carlsbad, CA) containing *Oatp1a1*, *Oatp1a4*, *Oatp1a5*, *Oatp1b2*, or *OATP1A2* cDNA was linearized with *NotI*. *OATP1C1*, *OATP3A1_v1*, or *OATP3A1_v2* in the *X. laevis* expression vector (4) (pSPORT1 that contains the initiation codon and the 5' as well as the 3'-UTR of *Oatp1a1* for efficient stability and expression of the cRNA) were linearized with *NotI*. Capped cRNA was synthesized using the mMESSAGE mMACHINE T7 kit (Ambion, Austin, TX). *X. laevis* oocytes were prepared by liberase digestion as previously described (15). After an overnight incubation at 18°C, healthy oocytes were microinjected with 50 nl water or with 5 ng cRNA in the same volume and kept in culture at 18°C for 3 days with daily change of medium before uptake of radiolabeled substrates was measured.

Transport assay in *X. laevis* oocytes. Uptake of radiolabeled substrates was measured at 25°C in 100 µl of uptake buffer (in mM: 100 NaCl or 100 choline chloride, 2 KCl, 1 MgCl₂, 1 CaCl₂, and 10 HEPES adjusted to pH 6.5 or 8.0 with Tris) as detailed in Reichel

et al. (47). In brief, 10 to 12 oocytes were prewashed in uptake buffer and incubated for 20 min in the same solution containing the radio-labeled substrate. After the oocytes were rinsed three times with ice-cold uptake buffer without radiolabeled substrate, oocytes were dissolved in 10% SDS for ³H-labeled substrates, 4 ml of scintillation liquid (Ultima Gold; Perkin-Elmer, Boston, MA) was added, and radioactivity was measured in a Packard Tri-Carb 2200 CA liquid scintillation analyzer (Canberra Industries, Meriden, CT). [¹²⁵I]T₄ was measured in intact oocytes in a Packard Cobra QC Auto-Gamma Counter (Canberra Industries).

Stably transfected cells. CHO-K1 and Madin-Darby Canine Kidney (MDCK) cells stably transfected with rat *Oatp1a1*, *OATP1B3*, *OATP1C1*, *OATP2B1*, or rat *Oatp1a5* were previously described (6, 13, 44, 45, 60, 62). CHO-K1 cells were grown in DMEM supplemented with 10% FCS, 50 µg/ml L-proline, 100 U/ml penicillin, and 100 µg/ml streptomycin. Selective medium for stably transfected CHO-K1 cells contained additionally 500 µg/ml geneticin sulfate (G418). MDCK cells stably expressing *Oatp1a5* were kindly provided by Dr. Paul A. Dawson [Wake Forest University, NC (62)]. They were maintained in DMEM supplemented with 10% FCS, 100 U/ml penicillin, and 100 µg/ml streptomycin, whereas selective medium contained additionally 350 µg/ml G418 (62). CHO FlpIn cells (FlpIn CHO-K1) were grown in Ham's F12 medium supplemented with 10% FCS, 1 mM L-glutamine, and zeocin (100 µg/ml). All cells were kept at 37°C with 5% CO₂ and 95% relative humidity.

FlpIn CHO-K1 cells stably transfected with rat *Oatp1a1*, *Oatp1a1* H107Q, rat *Oatp1b2*, *OATP1C1*, and *OATP1C1* Q130H were generated using the FlpIn recombinase-mediated system kit (Invitrogen, Carlsbad, CA), which permits the targeted integration of genes to the same locus in all transfected cells to provide a homogeneous level of gene expression. FlpIn CHO-K1 were cotransfected with the *Oatp/OATP*-containing plasmid and pOG44 that encodes the Flp recombinase by treatment with Lipofectamine 2000 (Invitrogen), and stably transfected cells were selected with hygromycin (500 or 600 µg/ml). In the case of stably transfected rat *Oatp1a1*-, *Oatp1a1* H107Q-, *OATP1C1*-, and *OATP1C1* Q130H-CHO FlpIn cells, single clones were isolated from the resulting transfected cell pools by limited dilution and tested for E3S or T₄ uptake. Clones exhibiting the highest transport activities were expanded and used in all experiments.

Transport assays in cells. Determination of substrate uptake into *Oatp/OATP* expressing CHO-K1 and MDCK cells was performed as described (6, 55, 62). Briefly, cells were grown to confluency on 35-mm dishes. Expression of *Oatp/OATP* was induced by incubation of the cells for 24 h with culture medium supplemented with 5 mM (CHO-K1 cells) or 10 mM (MDCK cells) sodium butyrate (43). At the day of the experiment, CHO-K1 cells on individual dishes were rinsed two times with prewarmed (37°C) uptake buffer (in mM: 116 choline chloride, 5.3 KCl, 1.1 KH₂PO₄ or NaH₂PO₄, 0.8 MgSO₄, 5.5 D-glucose, and 20 HEPES), whereas MDCK cells were rinsed with prewarmed PBS. Uptake experiments were performed in the uptake buffer (CHO-K1 cells) or in Hanks' balanced salt solution (for MDCK cells, in mM: 137 NaCl, 5.3 KCl, 0.46 KH₂PO₄, 0.27 Na₂HPO₄, 5.5 D-glucose, and 4.17 NaHCO₃) containing 0.15 µCi/ml ([¹²⁵I]thyroxine) or 0.2 to 1.2 µCi/ml (³H-labeled compounds) radiolabeled substrate supplemented with unlabeled compound to reach the indicated concentrations. Transport was stopped with 2 ml of ice-cold uptake buffer (CHO-K1) or PBS (MDCK) followed by two additional washes. Thereafter, cells were solubilized in 1 ml of 1% (wt/vol) Triton X-100 (CHO-K1) or 0.1 M NaOH (MDCK), and the radioactivity was measured by liquid scintillation counting. Protein concentrations on individual dishes were determined using the bicinchoninic acid protein (BCA) assay kit (Interchim, Montluçon Cedex, France) (56). Specific *Oatp/OATP*-mediated uptake was determined by subtracting values from identical experiments conducted in wild-type or mock-transfected cells.

For the inhibition experiments with acetazolamide and amiloride, these compounds were added to the uptake buffers as indicated in

Figure 6. To test the influence of the histidine-specific reagent diethylpyrocarbonate (DEPC) (16) on transport, CHO-K1 cells grown on 35-mm dishes were first washed twice with prewarmed uptake buffer of pH 7.4, incubated with different concentrations of DEPC in the uptake buffer (control without DEPC) for 10 min at 37°C and 5% CO₂, followed by the uptake procedure outlined above.

For kinetic analysis, the Michaelis-Menten constant (K_m) and maximal velocity (V_{max}) was calculated using nonlinear regression analysis (Systat Version 8.0, SPSS, Chicago, IL).

pH_i measurements. For intracellular pH (pH_i) measurements in CHO-K1 cells, the cells were grown to subconfluency on glass coverslips. For the duration of the experiment, they were kept in a thermostatically controlled chamber maintained at 37°C on an inverted microscope (Zeiss Axiovert 200) equipped with a video imaging system (64). The cells were incubated for 10 min with 10 μM of the pH-sensitive dye 2',7'-bis-(2-carboxyethyl)-5-(and 6)-carboxy-fluorescein (BCECF)-AM (48) (Invitrogen) in a HEPES-buffered Ringer solution (in mM: 125 NaCl, 5 KCl, 1 CaCl₂, 1.2 MgSO₄, 2 NaH₂PO₄, 32.2 HEPES, and 5 D-glucose, pH 7.4) at 37°C. For data presented in Fig. 5, A and B, wild-type CHO-K1 cells were then washed with buffer A (HCO₃⁻ containing/Cl⁻ containing; see Table 1) to remove extracellular non-deesterified BCECF-AM and to achieve a stable baseline, followed by buffer B (HCO₃⁻ free/Cl⁻ free) to induce an intracellular alkalinization. For one batch of cells, buffer C (HCO₃⁻ free/Cl⁻ containing) was added after the intracellular alkalinization to recover pH_i. For data presented in Fig. 5C, wild-type CHO-K1 cells were rinsed with buffer A (HCO₃⁻ containing/Cl⁻ containing; see Table 1) until a stable baseline was achieved, followed by superfusion with buffer D (HCO₃⁻ containing/Cl⁻ free; see Table 1) to induce intracellular alkalinization. Thereafter, cells were again superfused with buffer A. After completion of this incubation sequence, the same cells were again subjected to the described buffer changes, but all buffers were supplemented with 100 μM DIDS. For experiments shown in Fig. 7, cells were washed with buffer B (HCO₃⁻ free/Cl⁻ free) or buffer D (HCO₃⁻ containing/Cl⁻ free) after the BCECF-AM incubation. Both buffers contained additionally 0.1 mM acetazolamide, an inhibitor of the enzyme carbonic anhydrase (CA), and 1 mM of the sodium-proton exchanger inhibitor amiloride. After washing was completed, cells were superfused with the respective buffers for 10–15 min in the absence of any transporter substrates to obtain a stable baseline. E3S or TC (100 μM) were then added to the respective buffers, and cells were superfused for ~10 min to activate transport. During all experiments, cells were alternately excited at 490 and 440 nm, whereas the fluorescence emission was recorded at 535 nm every 5 s. The resulting 490/440 intensity ratio data were converted to pH_i by using the high K⁺/nigericin calibration technique

(50, 64). In brief, at the end of each experiment, an in situ calibration procedure with nigericin, a H⁺/K⁺ exchanger, was used to relate the fluorescence intensities to pH value. This H⁺/K⁺ exchanger ionophore sets $[K^+]_o = [K^+]_i$ and pH_o = pH_i by exposing the cells to different pH buffers in a depolarizing high K⁺ buffer (105 mM KCl, 1.2 mM MgSO₄, 32.8 mM N-methyl-D-glucamine, 1 mM CaCl₂, 32.2 mM HEPES, pH 6.5 and pH 7.0, in the presence of 10 μM nigericin).

Initial slopes after the addition of the substrates were calculated, and data were expressed as acidification (–pH_i/min) or alkalinization (+pH_i/min) rates, respectively. pH_i of ~19 single cells was recorded per experiment, and all experiments repeated with at least four batches of cells (total of 67–136 cells).

Statistical analysis. Values are shown as means ± SD (Figs. 1, 3, 4, 6) or as means ± SE (Fig. 7, Table 2). In transport experiments, statistical significance was determined by an unpaired Student's *t*-test. For comparison of K_m and V_{max} values in Table 2, a paired Student's *t*-test was performed when more than three experiments were done, whereas in the case of single or duplicate experiments, 95% confidence intervals are given in parenthesis. The software program GraphPad Prism Version 4.00 was used for nonlinear regression and statistical analysis (GraphPad Software, San Diego, CA).

RESULTS

Effect of extracellular pH on Oatp/OATP-mediated substrate transport. First, the effect of the extracellular pH on the transport activity of four rat Oatps and nine human OATPs expressed in *X. laevis* oocytes was investigated. For this, we chose the two prototypical substrates TC and E3S, which are transported by most Oatps/OATPs, and their uptake was measured in extracellular buffers of pH 6.5 and pH 8.0. Because some human OATPs are known to exhibit only low TC- or E3S-transport activity, we measured in addition uptake of PGE₂ (17, 57) and T₄ for some additional OATPs (8, 37, 44). All rat Oatps as well as human OATP1A2 and 1B3 displayed statistically significantly increased TC transport at extracellular pH 6.5 compared with extracellular pH 8.0, whereas human OATP1B1, OATP1C1, and all tested members of the OATP families 2 to 4 did not reveal any stimulation of TC transport at low extracellular pH (Fig. 1A). In contrast, E3S uptake at extracellular pH 6.5 was enhanced in all investigated Oatps/OATPs with the exception of the human OATP1B1 (Fig. 1B). For PGE₂, we observed significantly higher transport activity at extracellular pH 6.5 compared with pH 8.0 in all studied rat Oatps and human OATP1A2 and OATP1B1. Interestingly, also OATP1C1, OATP2B1, and OATP3A1_v1/_v2 tended toward increased PGE₂ transport at extracellular pH 6.5 (Fig. 1C). When T₄ was used as substrate, uptake was stimulated in all investigated Oatps/OATPs with the exception of rat Oatp1b2 and human OATP1C1 (Fig. 1D). It is interesting to note that with none of the substrates tested in Fig. 1, OATP1C1 displayed significant pH-sensitive transport activity, indicating that OATP1C1 has a transport mechanism different from the other OATPs/Oatps investigated. The activation of Oatp/OATP-mediated transport at low extracellular pH suggests either an Oatp/OATP-mediated transport associated with HCO₃⁻ (or OH⁻) exchange or with H⁺ cotransport. This should be reflected by a difference in V_{max} values at the two different pHs. Alternately, substrate binding to the transporter might be pH sensitive, which in turn would lead to a pH dependency of the respective apparent K_m values.

Table 1. Composition of buffers for pH_i measurements

	Buffer			
	A	B	C	D
KCl	5.3		5.3	
K-gluconate		5.3		5.3
NaH ₂ PO ₄ ·H ₂ O	1	1	1	1
MgSO ₄ ·7H ₂ O	0.8	0.8	0.8	0.8
D-glucose	5.5	5.5	5.5	5.5
NaCl	101.4		116.4	
Na-gluconate		116.4		101.4
NaHCO ₃	25			25
HEPES		20	20	
Acetazolamide		(0.1)		0.1
Amiloride		(1)		1
CO ₂ , %	5			5
O ₂ , %	95			95
pH	7.4	7.4	7.4	7.4

All solute concentrations are given in millimolar.

Table 2. pH dependency of Michaelis-Menten parameters of OATPs/Oatps

Substrate	pH 8.0		pH 6.5		n
	K_m , μM	V_{\max} , pmol/mg protein \cdot min $^{-1}$	K_m , μM	V_{\max} , pmol/mg protein \cdot min $^{-1}$	
Oatp1a1					
CHO					
E ₃ S	39.0 ± 4.3* (30.3 to 47.6)	1,689 ± 68.3 (1,553 to 1,826)	20.4 ± 2.7* (14.9 to 25.8)	1,529 ± 63.4 (1,402 to 1,655)	4
TC	79.4 ± 17.0* (45.5 to 113)	710 ± 58 (594 to 827)	31.7 ± 6.4* (19.0 to 44.4)	617 ± 37.5 (542 to 692)	5
Oatp1a5					
MDCK					
E ₃ S	177 ± 124 (−81.1 to 434)	453 ± 98.1 (250 to 657)	83.5 ± 45.0 (−9.85 to 177)	383 ± 50.4 (278 to 487)	2
TC	18.2 ± 3.0 (11.7 to 24.70)	46.6 ± 2.9 (40.3 to 52.9)	8.5 ± 2.8 (2.55 to 14.5)	55.1 ± 5.43 (43.4 to 66.8)	1
PGE ₂	108 ± 18.8 (69.1 to 148)	98.2 to 9.22 (78.9 to 117)	56.8 ± 11.5 (32.4 to 81.3)	85.1 ± 8.7 (66.6 to 104)	1
Oatp1b2					
CHO					
E ₃ S	91.7 ± 17.3 (57.2 to 126)	2,332 ± 206 (1,920 to 2,744)	56.1 ± 15.3 (25.5 to 86.6)	2,164 ± 232.5 (1,699 to 2,628)	5
TC	41.1 ± 9.8 (20.7 to 61.5)	475 ± 55.7 (360 to 591)	22.3 ± 5.71 (10.5 to 34.2)	407 ± 43.8 (316 to 498)	2
PGE ₂	20.0 ± 5.57 (8.56 to 31.5)	205 ± 26.1 (151 to 259)	9.57 ± 2.94 (3.50 to 15.6)	230 ± 26.1 (176 to 284)	2
OATP1B3					
CHO					
E ₃ S	73.0 ± 24.6 (23.7 to 122)	1,776 ± 370 (1,036 to 2,517)	54.6 ± 7.62 (39.3 to 69.8)	1,798 ± 133.3 (1,532 to 2,065)	3
OATP1C1					
CHO					
T ₄	0.18 ± 0.04 (0.10 to 0.26)	22.0 ± 1.91 (18.2 to 25.9)	0.27 ± 0.07 (0.13 to 0.40)	37.8 ± 4.72 (28.2 to 47.4)	2
OATP2B1					
CHO					
E ₃ S	17.8 ± 2.92 (11.8 to 23.8)	1,400 ± 114 (1,167 to 1,633)	9.36 ± 0.93 (7.46 to 11.3)	1,293 ± 51.13 (1,187 to 1,398)	2
T ₄	0.77 ± 0.18 (0.40 to 1.15)	7.28 ± 1.10 (5.04 to 9.51)	0.31 ± 0.09 (0.13 to 0.50)	5.76 ± 0.80 (4.13 to 7.39)	2

Values are means ± SE of 1–5 individual determinations (*n*). 95% confidence intervals are given in parentheses. Oatps, rodent organic anion transporting polypeptide; OATPS, human organic anion transporting polypeptide; CHO, chinese hamster ovary; MDCK, Madin-Darby canine kidney cells; E₃S, estrone-3-sulfate; TC, taurocholate; PGE, prostaglandin E₂; T₄, thyroxine; K_m , Michaelis-Menten constant; V_{\max} , maximal velocity. Wild-type CHO-K1 resp. MDCK cells or stably transfected CHO-Oatp1a1, -Oatp1b2, -OATP1B3, -OATP1C1, -OATP2B1, or MDCK-Oatp1a5 cells were grown to confluency on 35-mm dishes. After a 24-h incubation in 5 mM (CHO) or 10 mM (MDCK) sodium butyrate, the cells were incubated with increasing concentrations of radiolabeled substrates at 37°C for 15 s (CHO) resp. 1 min (MDCK) in a choline chloride medium. The net Oatp/OATP-mediated uptake values were calculated by subtracting the values obtained with the wild-type CHO-K1 resp. MDCK cells from those obtained with the stably transfected cells. Kinetic parameters were calculated by fitting the data to the Michaelis-Menten (K_m) equation with nonlinear regression. T₄, thyroxine. K_m values in bold and marked with an asterisk are significantly different ($P < 0.05$) between pH 6.5 and pH 8.0.

Therefore, we next determined the Michaelis-Menten parameters at extracellular pH 6.5 and pH 8.0 for E₃S, TC, PGE₂, and T₄ for selected rat and human Oatps/OATPs stably expressed in CHO-K1 and MDCK cells. In pilot experiments initial linear uptake rates of 15 s for OATP/Oatps in stably transfected CHO-K1 cells and of 1 min for rat Oatp1a5 expressed in MDCK cells were determined (data not shown).

We found that with the exception of OATP1C1-mediated T₄-uptake, all investigated Oatps/OATPs showed a tendency to decreased apparent K_m values at extracellular pH 6.5 compared with extracellular pH 8.0, whereas the V_{\max} values remained unaffected (Table 2). Statistical analysis showed that the apparent K_m values for Oatp1a1-mediated E₃S and TC uptake are significantly decreased at extracellular pH 6.5 compared with pH 8.0, whereas the V_{\max} values exhibited no significant differences between pH 6.5 and H 8.0 (Table 2).

Lower K_m values at acidic pH may be due to a higher affinity of the substrate to the respective transporter, which in turn may depend on the protonation state of the substrate used or on pH-dependent alterations of the binding site of the transport protein. To this end, it is interesting to note that one highly conserved histidine residue (His), which is located at the extracellular side of the third transmembrane domain (TMD), is replaced by a glutamine (Gln) residue in OATP1C1 (Fig. 2). Histidine has a pK_a of 6.9 in proteins (38). Therefore, it is likely that lowering the extracellular pH from 8.0 to 6.5 leads to protonation of the imidazole ring and consequently to the

addition of a positive charge to this conserved His (Fig. 2) in the analyzed Oatps/OATPs.

Influence of DEPC on transport activities of Oatps/OATPs. To investigate whether this conserved His in the third TMD (Fig. 2) indeed plays a role in the pH dependency of Oatp/OATP-mediated transport, uptake experiments in stably transfected CHO-K1 cells were performed in the absence and presence of the His-specific reagent DEPC (38). For this purpose, CHO-Oatp1a1, -Oatp1b2, -OATP2B1, and -OATP1C1 cells were preincubated for 10 min with different concentrations of DEPC or buffer only, followed by uptake measurements at 1 min using extracellular buffers of pH 6.5 and 8.0, respectively. Figure 3 shows that the pH dependency in the case of Oatp1a1- (Fig. 3A), Oatp1b2- (Fig. 3B), and OATP2B1-mediated (Fig. 3C) E₃S uptake was gradually reduced or even abolished with increasing DEPC concentrations at both pH values. OATP1C1-mediated T₄ uptake in contrast was not affected by DEPC at pH 6.5 (Fig. 3D), whereas at pH 8.0 the lowest concentration of 0.5 μM DEPC led to an inhibition of uptake by ~55%, which remained constant at this level at higher DEPC concentrations. The sensitivity of OATP1C1 to DEPC at pH 8.0 is most likely due to the presence of additional His residues. In OATP1C1, H260 and H468 probably also face the extracellular milieu (14). The distinct DEPC sensitivity of OATP1C1 at acidic pH further supports the hypothesis that the conserved His in the third TMD might be involved in the pH-sensitive transport but does

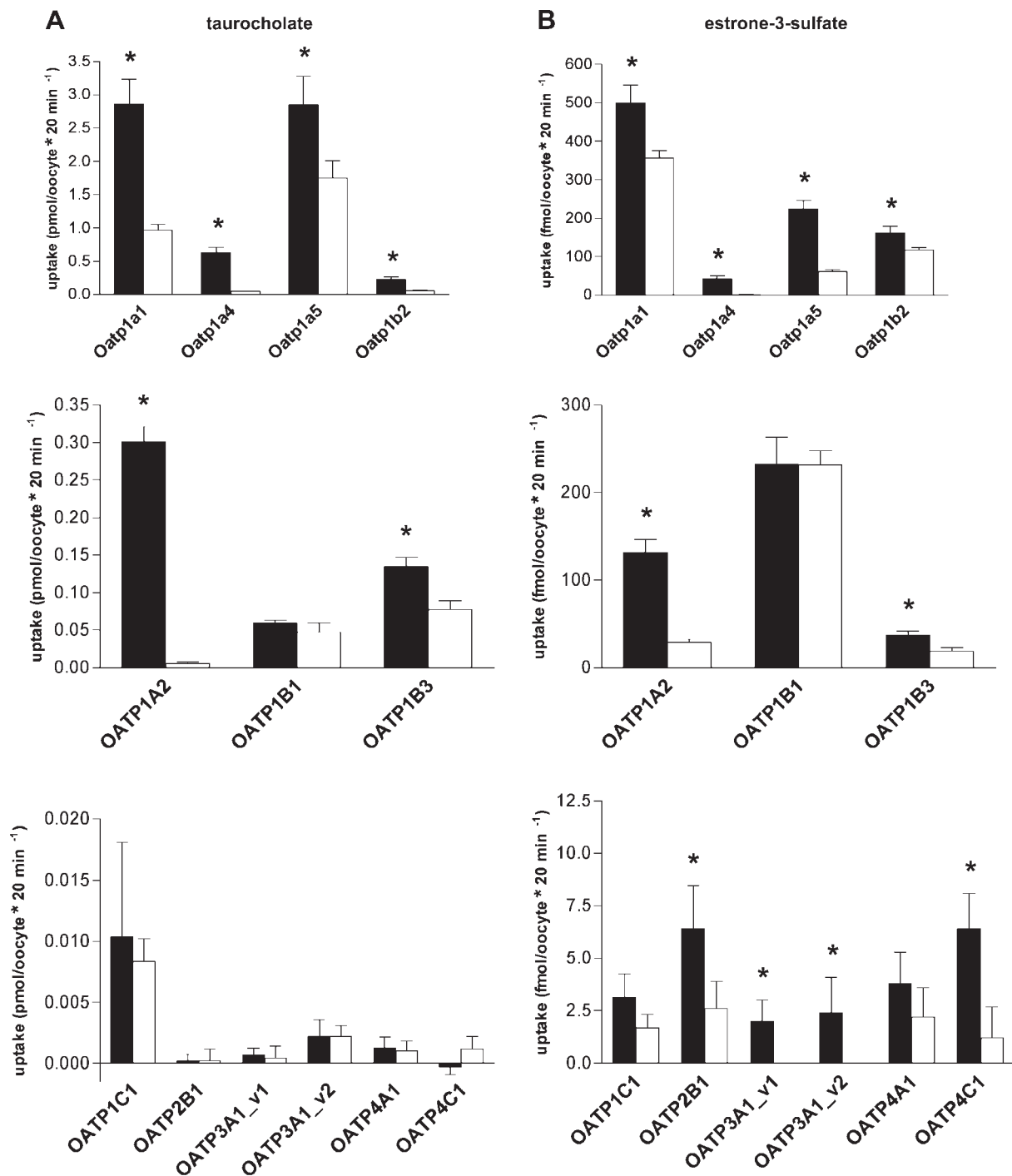


Fig. 1. Effect of extracellular pH on organic anion transporting polypeptides (rodent) Oatp/OATP (human)-mediated substrate transport in *Xenopus laevis* oocytes. Uptake of radiolabeled 5 μ M taurocholate (A), 0.5 μ M estrone-3-sulfate (B), 20 nM prostaglandin E₂ (C), and 10 nM thyroxine (D) was measured for 20 min at 25°C as described under MATERIALS AND METHODS. Black bars, extracellular pH 6.5; open bars, extracellular pH 8.0. Results are expressed as means \pm SD of 20–30 oocytes from 2–3 independent experiments (uptake values corrected for unspecific transport in water-injected oocytes). * $P < 0.05$.

not rule out a reaction of DEPC with other His residues present in the investigated OATPs/Oatps.

Effect of the conserved His in the third TMD on pH-sensitive Oatp1a1- and OATP1C1-mediated substrate transport. To specifically assess the potential involvement of the conserved His in the third TMD and to exclude an effect of other His residues in pH-sensitive substrate transport by OATPs/Oatps,

mutants were generated by exchanging Gln130 to a His in OATP1C1 (OATP1C1 Q130H) and His107 to a Gln in Oatp1a1 (Oatp1a1 H107Q). These mutants and wild-type Oatps/OATPs were stably expressed in FlpIn CHO-K1 cells, and uptake experiments were performed at extracellular pH 6.5 and pH 8.0. The pH sensitivity of Oatp1a1-mediated substrate transport (stimulation by $175 \pm 15.7\%$ at pH 6.5 vs. pH 8.0;

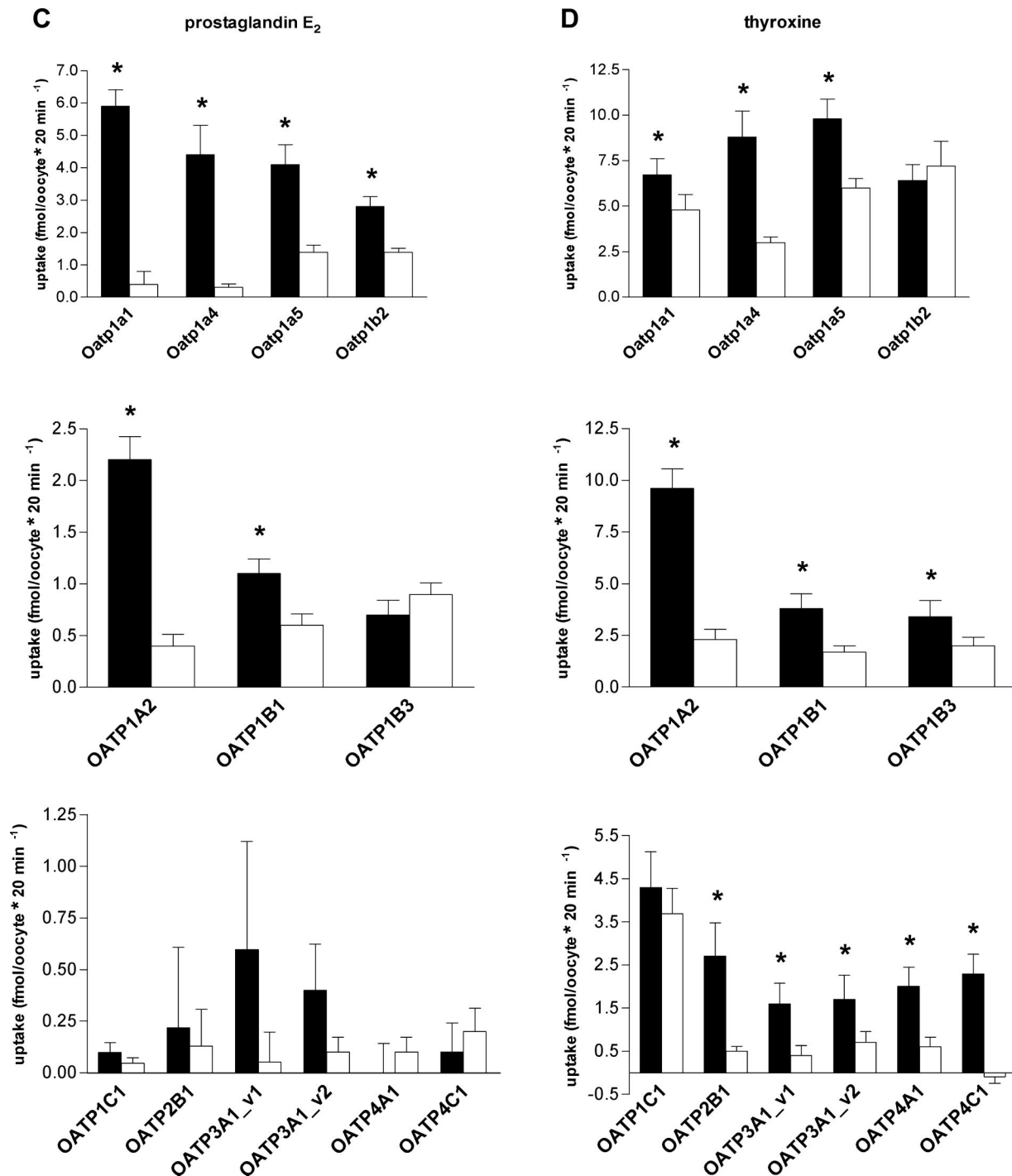


Fig. 1.—Continued

$P < 0.01$) disappeared in Oatp1a1 H107Q (Fig. 4A), whereas OATP1C1 Q130H-mediated T₄-uptake acquired pH sensitivity (stimulation by $115 \pm 39.3\%$ at pH 6.5 vs. pH 8.0; $P < 0.01$) in contrast to the wild-type OATP1C1 (Fig. 4B). This finding is a strong indication for the involvement of this highly conserved His in pH-sensitive substrate binding. These results together with the DEPC inhibition experiments strongly suggest that the highly conserved His in the third TMD plays a crucial role in the pH sensitivity of the apparent K_m values of Oatps/OATPs.

Influence of extracellular chloride on pH_i recovery of CHO-K1 cells. Despite the role of a His in OATP/Oatp-mediated transport, the results in Fig. 1 do not entirely exclude a potential role of bicarbonate as a counterion for substrate uptake. This assumption has been strongly supported for rat Oatp1a1 (54), implying taurocholate/bicarbonate exchange. Hence, we aimed to preload CHO-K1 cells transfected with OATPs/Oatps with bicarbonate and to determine bicarbonate efflux by online measurement of pH_i changes (64). To this end, we first verified the functional expression of a Cl⁻/HCO₃⁻

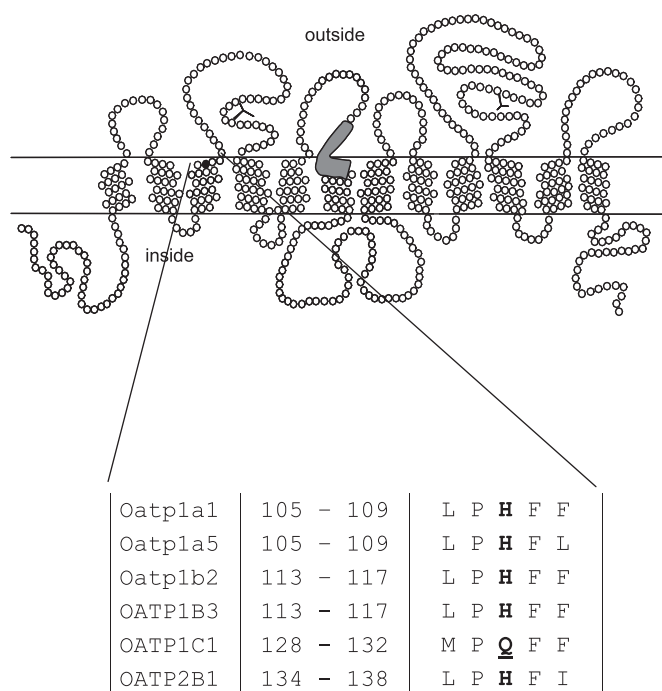


Fig. 2. Predicted 12 transmembrane domain model of an Oatp/OATP and amino acid sequence comparison of investigated Oatps/OATPs. *N*-glycosylation sites (Y) are present on extracellular protein loops. The OATP superfamily signature is indicated in grey at the border of the extracellular loop 3 and the TMD 6.

exchanger in CHO-K1 cells. The results in Fig. 5 demonstrate a rapid increase of pH_i after changing the incubation solution from a buffer containing 107 mM Cl^- and 25 mM HCO_3^- (Table 1, buffer A, pH 7.4) after equilibrating the cells for 5–10 min to a HEPES-buffered HCO_3^- free/ Cl^- free solution (Cl^- replaced by gluconate; Table 1, buffer B, pH 7.4). This procedure led to a rapid intracellular alkalinization as a result of the efflux of CO_2 from the cells (Fig. 5A). The rate of pH_i recovery was very low with $-0.0092 \pm 0.070 \Delta pH_i/\text{min}$ ($n = 17$). When extracellular Cl^- (122 mM) was added back to the incubation solution, the rate of pH_i recovery after the intracellular alkalinization was increased to $-0.0567 \pm 0.0041 \Delta pH_i/\text{min}$, $n = 19$ (Fig. 5B; Table 1, buffer C, pH 7.4), which was significant compared with the recovery rate in Fig. 5A ($P < 0.01$). Cl^-/HCO_3^- exchange is subject to inhibition by DIDS (46, 49). Therefore, we tested the influence of DIDS on the observed pH_i recovery after alkalinization (Fig. 5B). Figure 5, C and D, demonstrates that the pH_i recovery rate ($0.031 \pm 0.0012 \Delta pH/\text{min}$) was significantly reduced in the presence of DIDS [$0.013 \pm 0.0008 \Delta pH/\text{min}$ ($P < 0.01$)]. Taken together, these data clearly demonstrate the existence of a Cl^-/HCO_3^- exchanger in CHO-K1 cells, which could be used to load the cells with HCO_3^- .

Effect of amiloride and acetazolamide on Oatp/OATP-mediated transport activity. To eliminate any contribution to pH_i changes caused by CA or the sodium-proton exchanger (NHE) expressed in CHO-K1 cells and consequently minimizing pH_i changes from OATP/Oatp-mediated bicarbonate efflux, we added 0.1 mM acetazolamide, an inhibitor of CA (58), and 1 mM amiloride, an inhibitor of NHE (22, 51). To test a possible interference of these two inhibitors with Oatp/OATP-mediated

substrate transport, uptake of TC and E3S in stably transfected CHO-Oatp1a1 cells was measured in the absence and presence of amiloride or acetazolamide. Figure 6 shows that amiloride did not change transport activity for both substrates. In contrast, acetazolamide showed a significant inhibition of TC uptake by $25.1 \pm 10.0\%$ ($P < 0.05$), whereas E3S uptake was significantly stimulated by $19.4 \pm 3.2\%$ ($P < 0.05$). The effect of acetazolamide was deemed to be too small to interfere with the planned experiments, since the remaining transport activity of Oatp1a1 with TC as substrate is still 75%.

Effect of Oatp/OATP-mediated substrate transport on pH_i in stably transfected CHO-K1 cells. pH_i changes after the addition of TC or E3S were measured in wild-type and stably transfected CHO-K1 cells. Cells were superfused with buffer D (Table 1, HCO_3^- containing/ Cl^- free) or buffer B (Table 1, HCO_3^- free/ Cl^- free) during the experiment. Figure 7A shows acidification rates of wild-type and rat Oatp1a1-CHO cells HCO_3^- preloaded or not preloaded in response to exposure to 100 μM TC. pH_i changes differed significantly between HCO_3^- -preloaded wild-type and stably transfected cells ($P < 0.01$), whereas pH_i changes between not preloaded wild-type and stably transfected cells were not significantly different ($P = 0.18$). After wild-type acidification rates were subtracted from the values obtained from rat Oatp1a1-CHO cells, acidification rates of HCO_3^- -preloaded cells were significantly higher than acidification rates from unloaded cells (Fig. 7B; $P < 0.01$). These results are in line with the data from Satlin and co-workers (54) and confirm that rat Oatp1a1 mediates taurocholate/bicarbonate exchange. We went on to measure acidification rates of HCO_3^- -preloaded and not preloaded wild-type and rat Oatp1a1-, OATP1B3-, and OATP2B1-CHO cells after the addition of 100 μM E3S. Figure 7, C–E, shows rates of pH_i changes of stably transfected cells after subtracting wild-type values. In all investigated HCO_3^- -preloaded cells, acidification rates were significantly higher compared with acidification rates in unloaded cells (Fig. 7, C–E; $P < 0.01$). Hence, the three OATPs/Oatps investigated mediate E3S/bicarbonate exchange.

DISCUSSION

Since detailed information on the driving force(s) and on the transport mechanism(s) of Oatps/OATPs is scarce, we decided to further investigate the role of the extracellular pH on the transport activity of 11 rat and human Oatps/OATPs. These experiments yielded three main findings. First, with the exception of OATP1C1, all investigated OATPs/Oatps displayed increased transport activity for different substrates under conditions of low compared with high extracellular pH. This finding was paralleled by a decreased apparent K_m value at low extracellular pH. Second, OATPs/Oatps have a conserved His in the third TMD possibly facing the extracellular milieu. This His residue is absent from the pH-insensitive OATP1C1, which upon introduction of a His at position 130 turns into a pH-sensitive transporter. Finally, substrate-mediated bicarbonate efflux was identified in all OATPs/Oatps documented by online intracellular pH determinations.

The stimulation of Oatp/OATP-mediated transport by an acidic extracellular pH was observed in both the amphibian *X. laevis* oocytes and the mammalian CHO-K1 cell expression systems (Fig. 1; Table 2). This observation clearly demon-

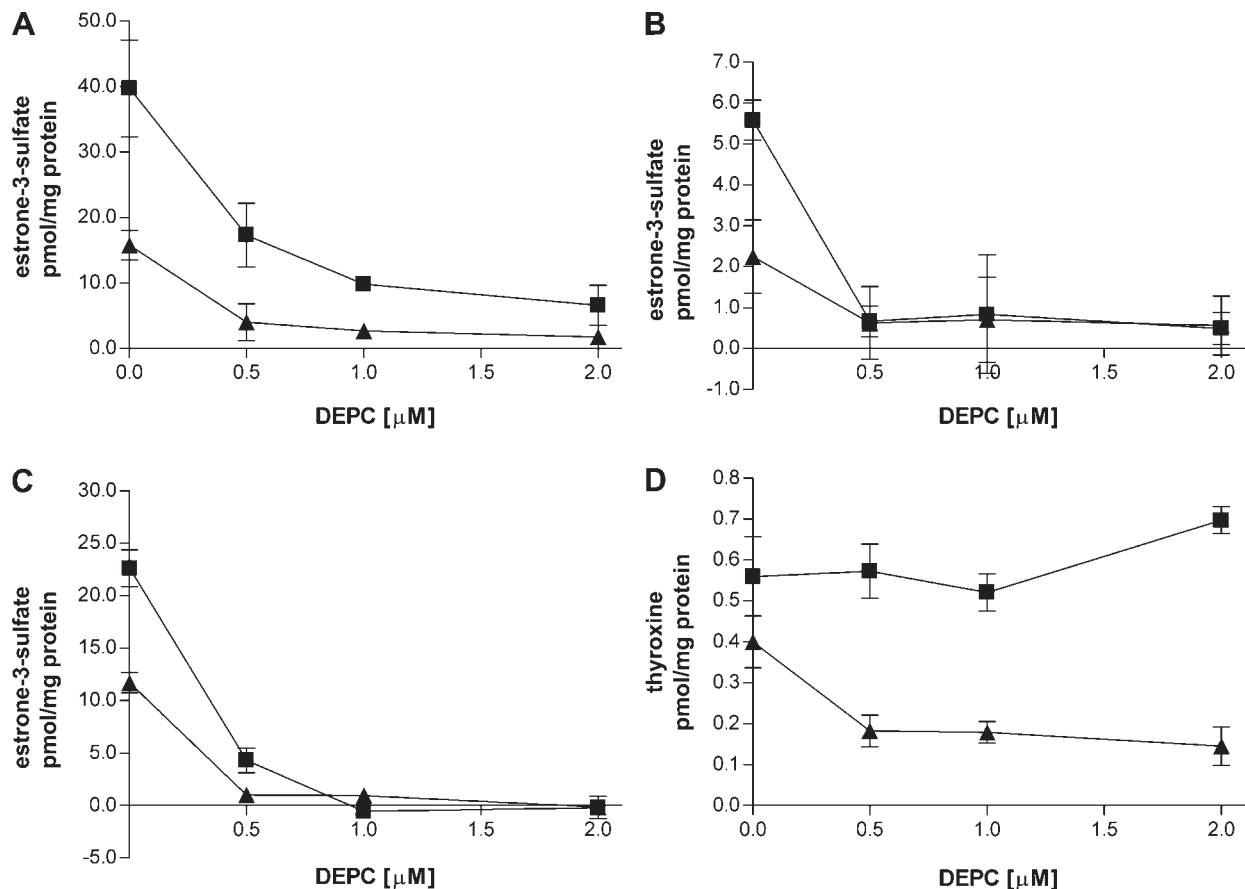


Fig. 3. Influence of diethylpyrocarbonate (DEPC) on transport activities of Oatps/OATPs in stably transfected CHO-K1 cells. Oatp1a1-mediated (A), Oatp1b2-mediated (B), and OATP2B1-mediated uptake of 0.5 μM estrone-3-sulfate (C), as well as OATP1C1-mediated uptake of 10 nM thyroxine (D) was determined after 10 min preincubation with increasing concentrations of DEPC or buffer only. Squares, extracellular pH 6.5; triangles, extracellular pH 8.0. Uptake values are corrected for unspecific transport in untransfected CHO-K1 cells and represent means \pm SD of triplicate determinations. Representative experiments of 3 independent transport studies are shown.

strates that stimulation of Oatp/OATP-mediated transport by an extracellular pH is an intrinsic property of the transporters and not related to the expression system used for transporter characterization. This conclusion is further supported by previous studies of the effect of extracellular pH on Oatp/OATP-mediated substrate transport in HeLa-Oatp1a1, CHO-Oatp1a1, and HEK293-OATP2B1 cells using different approaches (20, 23, 34, 39, 42, 52, 54). Thus our data are in line with all these studies showing an enhanced OATP/Oatp-mediated substrate transport in the presence of a low extracellular pH. Of all the OATPs/Oatps investigated, OATP1B1 showed no pH dependency for TC and E3S, while transport of PE2 and T₄ uptake into *X. laevis* oocytes was stimulated by a low extracellular pH (Fig. 1). This finding may be explained by the observation that OATP1B1 has two binding sites for E3S with apparent K_m values of 0.23 and 45 μM, respectively, but only one for fluvastatin (41). Thus it can be speculated that only one of the two E3S binding sites is pH sensitive. This site could be the binding site for T₄ and PGE₂. If this is the low-affinity E3S binding site, we might have missed the pH dependency at the E3S concentration used in our study. Marin and coworkers (34) investigated the effect of different transmembrane pH gradients on GC transport in stably transfected CHO-Oatp1a1 cells by changing the intracellular pH with amiloride, NH₄Cl, or imidazole. They also observed that GC uptake was higher in the

presence of an inwardly compared with an outwardly directed H⁺ gradient. However, this stimulation was not proportional to the magnitude of the gradient. These authors suggested that changes in pH_i triggers a modification of the protonation state of intracellular domains of the transport protein and, therefore, cause the changes in transport activity. Another study reported that the proton ionophore FCCP caused a significant reduction of OATP2B1-mediated E3S uptake at acidic extracellular pH in HEK-293 cells, suggesting that a proton gradient could be a driving force for OATP2B1 (42). Sai and coworkers (52) expressed OATP2B1 in HEK-293 cells and demonstrated that an inwardly directed pH gradient enhanced transport of E3S into vesicles isolated from these cells.

Changing the extracellular pH of an expression system can either affect the protonation state and consequently the charge of the substrate and/or the substrate binding pocket of the transporter investigated. Our kinetic analysis of Oatp/OATP-mediated substrate transport in stably transfected CHO-K1 and MDCK cells revealed that extracellular low pH leads to an increase of the apparent affinity (decreased K_m value) with no marked effect on V_{max} for all Oatps/OATPs studied except for OATP1C1 (Table 2). Whereas only the data for Oatp1a1 reached statistical significance, all other OATPs/Oatps (with the exception of OATP1C1) showed an increase in apparent affinity. Hence, we conclude that this pH dependency of

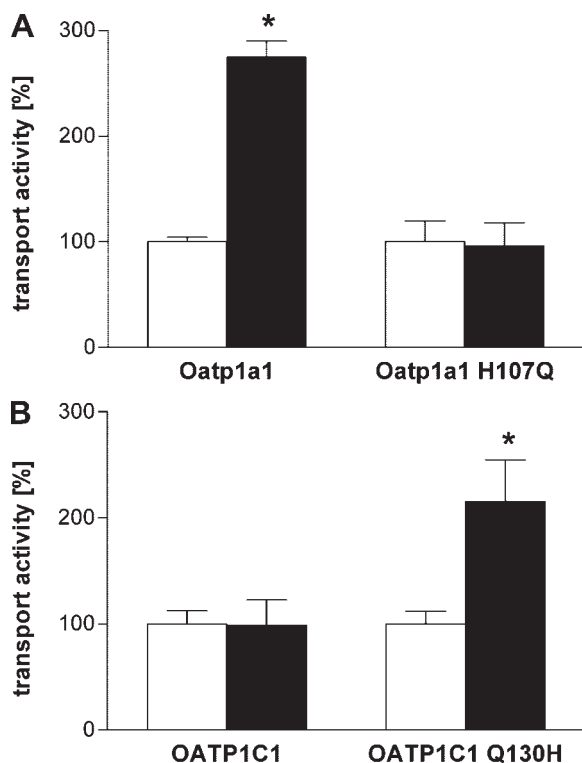


Fig. 4. Effect of the conserved His in the third transmembrane domain on pH-sensitive Oatp1a1- and OATP1C1-mediated transport in stably transfected CHO-K1 cells. Uptake of 0.5 μ M estrone-3-sulfate (Oatp1a1, Oatp1a1 H107Q) (A) or 10 nM thyroxine (OATP1C1, OATP1C1 Q130H) (B) was measured for 1 min at 37°C as described under MATERIALS AND METHODS. Solid bars, extracellular pH 6.5; open bars, extracellular pH 8.0. Results are expressed as means \pm SD of triplicate determinations from 3 independently performed transport studies. Uptake values are corrected for unspecific transport in CHO-K1 cells and normalized to uptake at pH 8.0 (= 100%). Absolute uptakes were for Oatp1a1: pH 6.5: 30.9 ± 10.9 pmol/mg protein·min, pH 8.0: 12.7 ± 7.07 pmol/mg protein·min; for Oatp1a1 H107Q: pH 6.5: 2.84 ± 1.27 pmol/mg protein·min, pH 8.0: 2.95 ± 1.24 pmol/mg protein·min; for OATP1C1: pH 6.5: 0.0917 ± 0.0809 pmol/mg protein·min, pH 8.0: 0.0897 ± 0.0779 pmol/mg protein·min for OATP1C1 Q130H: pH 6.5: 0.33 ± 0.146 pmol/mg protein·min, pH 8.0: 0.198 ± 0.073 pmol/mg protein·min, * $P < 0.01$.

apparent substrate affinities can be generalized for all investigated transporters but OATP1C1. Similar results were also obtained for the H^+ gradient-dependent peptide transporter PEPT1 in the small intestine, where lowering the extracellular pH leads to a decreased K_m while V_{max} remains unchanged (27, 61). In contrast to our findings, it was demonstrated that an acidic extracellular pH increases V_{max} without affecting K_m of OATP2B1-mediated E3S-transport in HEK293 cells (42). However, these authors used different extracellular pH settings (pH 5.0 vs. pH 7.4) and different incubation times for pH 5.0 and pH 7.4, which could contribute to this divergent finding. Furthermore, Marin and coworkers (34) observed that intracellular acidification leads to a decrease in V_{max} with no effect on K_m of Oatp1a1-mediated GC transport in CHO-K1 cells (34). Marin and coworkers also used CHO-K1 cells, but they modified the intracellular pH using amiloride without changing the extracellular pH (pH_i 7.45/pH_o 7.40 vs. pH_i 7.30/pH_o 7.40). These different experimental settings might account for the discrepancies to our data. However, when considering intrinsic clearances, defined as V_{max}/K_m , our data are consistent with the

findings of both groups. Intrinsic clearances at extracellular pH 6.5 were, with the exception of OATP1C1-mediated T₄-transport, 1.4- to 2.7-fold higher compared with extracellular pH 8.0 in our study (data not shown). Nozawa et al. (42) observed a 4.4-fold higher intrinsic clearance at extracellular pH 5.0 to extracellular pH 7.4, whereas Marin et al. (34) reported a 1.7-fold enhanced intrinsic clearance at intracellular pH 7.45 compared with intracellular pH 7.30.

The observed lower apparent K_m values at extracellular pH 6.5 reflect an increased affinity of the substrate to the transport protein. Because all tested substrates are predominantly present in their anionic form with a constant negative charge under the applied pH conditions, the protonation state of amino acids of the binding site of the transporters could be changed. Since His is an amino acid, which can alter the protonation state and consequently the charge of its side-chain, we searched the OATPs/Oatps for His residues near the extracellular side of the predicted 12 TMD structure and found a highly conserved His in the third TMD fulfilling this criterion (Fig. 2) His residues are known to play an essential role in pH-sensitive transporters (38). Interestingly, this His was absent from the third TMD of OATP1C1, which does not display pH-sensitive substrate transport. This fact in conjunction with the missing decrease of K_m in OATP1C1-mediated T₄-uptake at extracellular pH 6.5 (Table 2), allowed to test the hypothesis that this His in the third TMD might play an essential role in the pH sensitivity of Oatp/OATP-mediated substrate transport. Indeed, both experiments with transport in the presence of the His-modifying chemical DEPC and with the introduction of a His into the third TMD of OATP1C1 confirmed this hypothesis (Figs. 3 and 4). The significance of His residues was also shown for the H^+ gradient-dependent peptide transporters PepT1 and PepT2 in studies with renal and intestinal brush-border membrane vesicles, where transport activity was severely impaired following incubation with DEPC (21, 29). Other examples include the Na⁺/H⁺ exchanger (9, 12), the organic cation/H⁺ antiporter (16) or the folate transporter (53). In all these transporters, one or more individual His residue(s) were identified as important factors for transport activity (1, 7, 63). Recently, structural models for OATP1B3 and OATP2B1 were generated in silico, and a positively charged central pore was identified (36). Around this putative core, highly conserved single amino acid residues were found, which are thought to be responsible for the positive charge of the pore and most probably contribute to the substrate-binding site of the OATP1 and/or OATP2 family. Although no residue was identified to be fully conserved throughout the OATP/SLCO superfamily, a His in OATP2B1 was found to be conserved in all OATP2 family members. In the 12 TMD model of Oatps/OATPs, this His579 is located in TMD 10. As it is predicted to face the pore, it is exposed to the extracellular medium and therefore susceptible to pH changes of the medium. His92 in OATP1B3 is highly, although not fully conserved among the OATP1 family and also faces the central pore. Hence, this study confirms that His residues play an important role in the substrate-binding sites of Oatps/OATPs. In addition, Meier-Abt et al. (36) selected in their study the large extracellular loop 9–10 for a structural modeling attempt and found that the electrostatic potential of the loop is not positive. Therefore, they suggested that it might not be involved in the attraction of the substrate to the transporter but might cover the pore in the

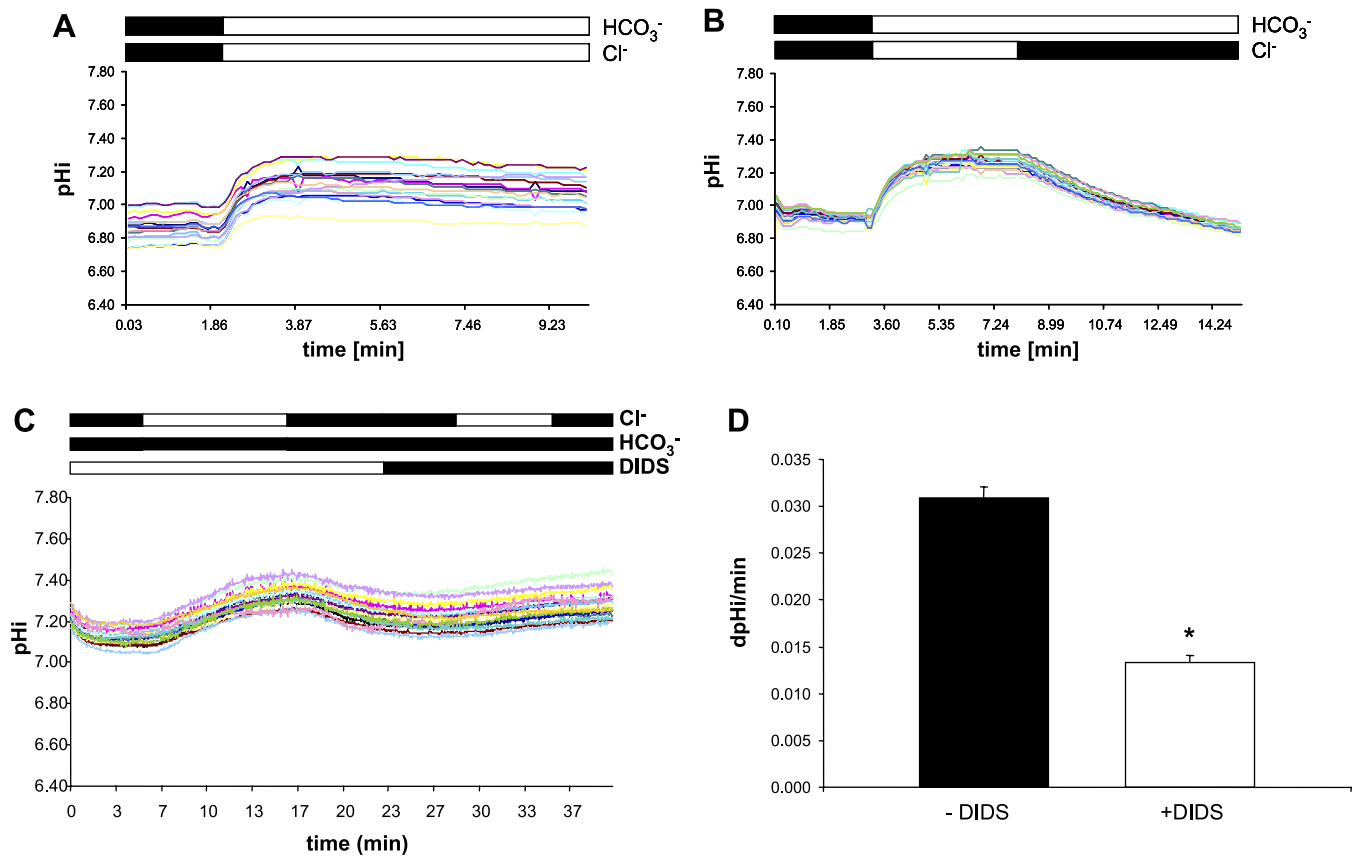


Fig. 5. Influence of extracellular chloride on pH_i recovery in wild-type CHO-K1 cells. A: pH_i recovery after acute intracellular alkalinization by CO₂ efflux in the absence of extracellular Cl⁻. Cells were superfused with buffer A (HCO₃⁻ containing/Cl⁻ containing) for ~5 min, before the incubation buffer was exchanged for buffer B (HCO₃⁻ free/Cl⁻ free). B: pH_i recovery after acute intracellular alkalinization by CO₂ efflux in the presence of extracellular Cl⁻. After intracellular alkalinization, buffer C (HCO₃⁻ free/Cl⁻ containing) was added to induce pH_i recovery. C: influence of DIDS (100 μM) on intracellular alkalinization rates. After reaching a steady state, cellular alkalinization was started by HCO₃⁻ containing/Cl⁻ containing buffer (buffer D) first in the absence and then in the presence of DIDS. D: effect of DIDS on intracellular alkalinization rates. Initial slopes after removal of chloride from the incubation solution were determined. Alkalinization rates are given as (+pH_i/min) in means ± SE as described under MATERIALS AND METHODS. Buffer conditions are indicated by the bars above the figure. Solid indicates the presence, open indicates the absence of the respective anion. Representative tracings of pH_i of individual cells are shown. *P < 0.01.

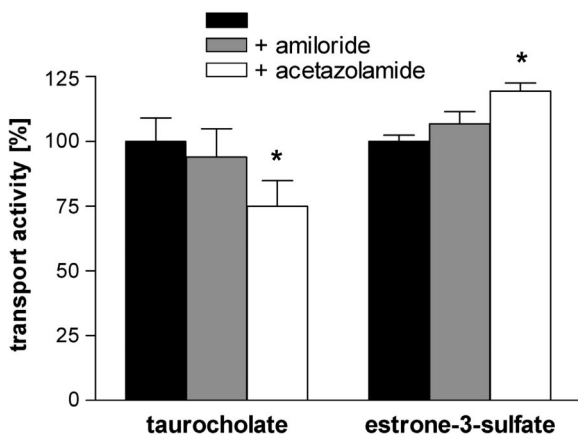


Fig. 6. Effect of amiloride and acetazolamide on transport activity of Oatp1a1 in stably transfected CHO-K1 cells. Uptake of 10 μM taurocholate and 0.5 μM estrone-3-sulfate was measured in the absence of any inhibitor (solid bars), in the presence of 1 mM amiloride (shaded bars) or 0.1 mM acetazolamide (open bars) for 30 s at 37°C as described under MATERIALS AND METHODS. Uptake values are corrected for unspecific transport in CHO-K1 cells and normalized to uptake without any inhibitor (= 100%). Results are expressed as means ± SD of triplicate determinations of 2 independently performed transport studies. *P < 0.05.

absence of substrate, moving away after substrate binding. Finally, investigations on the role of polymorphisms of OATPs on OATP-mediated substrate transport revealed a clustering of nonsynonymous polymorphisms in the third and fourth TMD as well as the extracellular loop connecting these TMDs (26), many of which lead to altered transport functions (65). These findings highlight again a potential role of the third TMD and its adjacent elements in OATP/Oatp-mediated substrate transport. To the best of our knowledge, no polymorphisms of the conserved His in the third TMD have been described so far, which also supports the importance of this His in the transport mechanism of OATPs/Oatps.

Increasing the extracellular H⁺ concentration will lead to a conversion of HCO₃⁻ and H⁺ into H₂O and CO₂, causing an outwardly directed HCO₃⁻ gradient across cell membranes. This in turn might facilitate OATP/Oatp-mediated substrate uptake into cells. Therefore, we investigated the capacity of extracellular substrates of Oatps/OATPs to stimulate HCO₃⁻ efflux in stably transfected HCO₃⁻-loaded CHO-K1 cells. We chose to monitor the intracellular pH online, which inversely correlates with intracellular bicarbonate concentration. We could demonstrate in CHO-K1 cells the presence of a Cl⁻/HCO₃⁻ exchanger (Fig. 5) and substrate induced bicarbonate

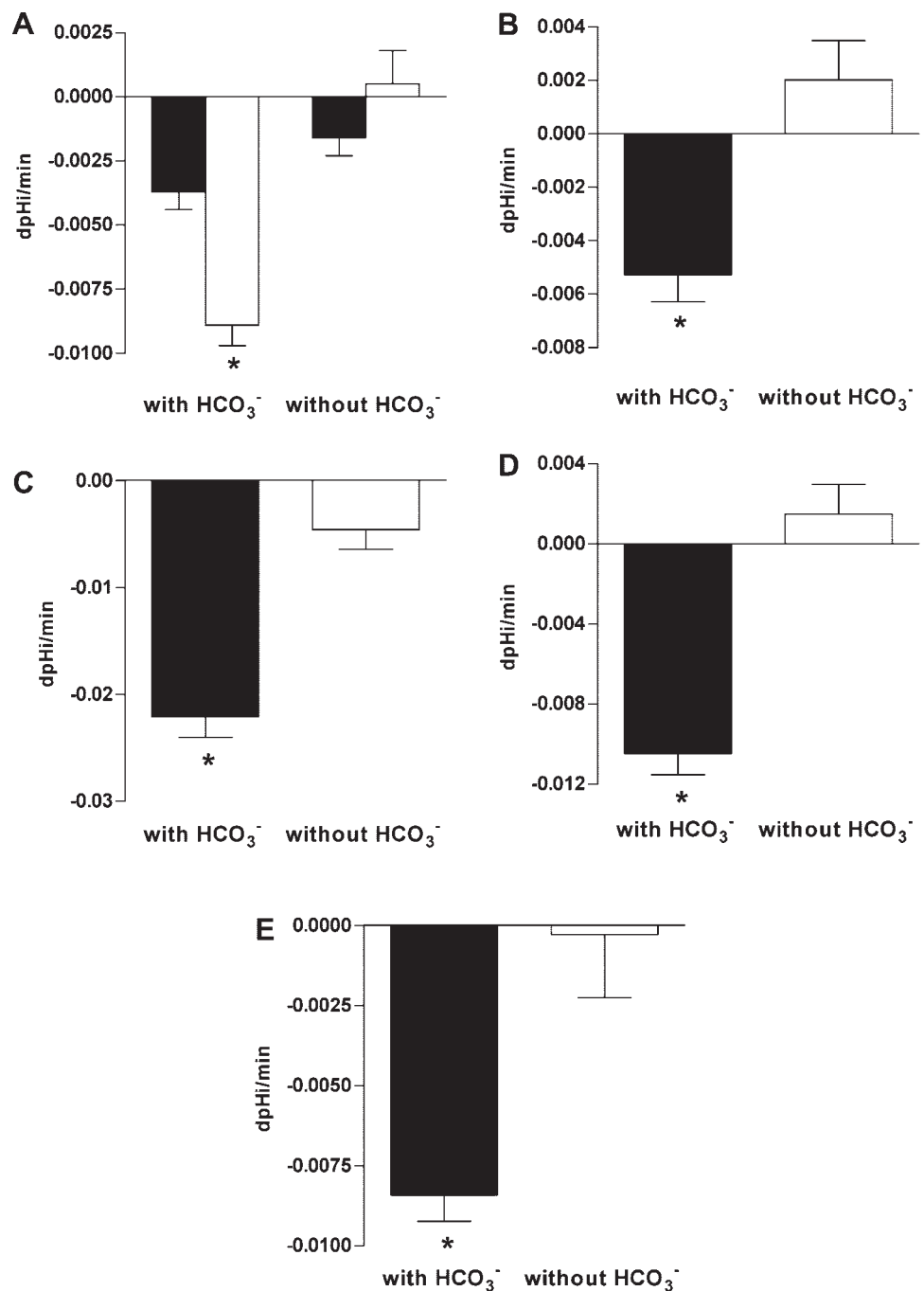


Fig. 7. Acidification rates in HCO_3^- preloaded and unloaded Oatp1a1- (A–C), OATP1B3- (D), OATP2B1-transfected CHO-K1 (E) or wild-type CHO-K1 cells induced by 100 μM taurocholate (TC) (A–B) or 100 μM estrone-3-sulfate (E3S) (C–E). Cells were superfused with a HCO_3^- -containing or HCO_3^- -free buffer before TC or E3S was added. Initial slopes after the addition of the substrates were calculated, and data were expressed as acidification rates ($-\text{pH}_i/\text{min}$) in means \pm SE as described under MATERIALS AND METHODS. In A, solid bars indicate wild-type, open bars indicated stably transfected Oatp1a1-CHO cells. In B–E, differences in $-\text{pH}_i/\text{min}$ between wild-type and stably transfected CHO-K1 cells are shown for HCO_3^- -preloaded and unloaded cells. * $P < 0.01$.

efflux from OATP/Oatp expressing cells (Fig. 7). In the rat and human liver, Oatp1a1, OATP1B3, and OATP2B1 are expressed at the basolateral membrane of hepatocytes (6, 24, 31, 47). pH homeostasis in hepatocytes is established by the coordinate action of two acid extruders, the basolateral Na^+/H^+ exchanger and the $\text{Na}^+/\text{HCO}_3^-$ symporter, and one acid loader, the canalicular $\text{Cl}^-/\text{HCO}_3^-$ exchanger (3). Although the pH_i of hepatocytes is kept at ~ 7.2 in a narrow range (2) and therefore slightly more acidic than the portal blood (7.4), the outward movement of HCO_3^- may be favored by the outwardly directed HCO_3^- gradient established by the $\text{Na}^+/\text{HCO}_3^-$ symporter. In addition, the existence of an unstirred water layer and a proton diffusion barrier in the Disse space,

which is located between the basolateral membrane and the endothelial cell layer, was postulated (18). This proton diffusion barrier is thought to be a stagnant layer that acts as a diffusion barrier for proton transfer from the membrane surface to bulk water and exhibits therefore a lower pH compared with this bulk phase. The proton diffusion barrier in hepatocytes is probably maintained by the extrusion of protons by the Na^+/H^+ exchanger, the negative electric field exerted by anionic phospholipid head groups, the unstirred water layer, and the existence of extracellular matrix proteins such as fibronectin and collagen in the Disse space. In the small intestine, the existence of a region in proximity to the apical membrane of enterocytes with a lower pH compared with the

bulk phase of the lumen of the gut is well established (59). This region, which is known as the microclimate pH region, is created by the diffusion barrier in the mucus layer, the glyco-calix, and by proton secretion from the enterocytes, whereby the transport systems involved are still a matter of debate (59). Such local acidic pH microclimates in the liver and the small intestine are likely to create an inwardly directed H^+ gradient and therefore could well stimulate under physiological conditions transport activities of Oatps/OATPs expressed at these sites.

In conclusion, in the present study we have demonstrated that the transport activity of OATPs/Oatps is generally stimulated by an acidic extracellular environment. Additionally, OATP/Oatp substrate transport generally leads to stimulation of bicarbonate efflux, further supporting the concept that OATPs/Oatps act as anion exchangers. The pH dependency of OATPs/Oatps is linked to a highly conserved His in the third TMD, an area that is also involved in altered transport properties of polymorphic OATPs. Nevertheless, the exact identification of a substrate binding site(s) and/or other sites critically involved in substrate transport by OATPs/Oatps requires further studies.

ACKNOWLEDGMENTS

Present address for B. Hagenbuch: Dept. of Pharmacology, Toxicology and Therapeutics, University of Kansas, Medical Center, Kansas City, KS 66160-7417.

Present address for P. J. Meier: University of Basel, Petersgraben 35/3, 4003 Basel, Switzerland.

GRANTS

This study has been supported by the Swiss National Science Foundation Grants 31-64140.00 to P. J. Meier and 3100A0112524/1 to B. Stieger.

REFERENCES

- Asaka J, Terada T, Tsuda M, Katsura T, Inui K. Identification of essential histidine and cysteine residues of the H^+ /organic cation antiporter multidrug and toxin extrusion (MATE). *Mol Pharmacol* 71: 1487–1493, 2007.
- Benedetti A, Strazzabosco M, Corasanti JG, Haddad P, Graf J, Boyer JL. Cl^- - HCO_3^- exchanger in isolated rat hepatocytes: role in regulation of intracellular pH. *Am J Physiol Gastrointest Liver Physiol* 261: G512–G522, 1991.
- Boyer JL, Graf J, Meier PJ. Hepatic transport systems regulating pH_i, cell volume, and bile secretion. *Annu Rev Physiol* 54: 415–438, 1992.
- Cattori V, Hagenbuch B, Hagenbuch N, Stieger B, Ha R, Winterhalter KE, Meier PJ. Identification of organic anion transporting polypeptide 4 (Oatp4) as a major full-length isoform of the liver-specific transporter-1 (rlst-1) in rat liver. *FEBS Lett* 474: 242–245, 2000.
- Cattori V, van Montfort JE, Stieger B, Landmann L, Meijer DK, Winterhalter KH, Meier PJ, Hagenbuch B. Localization of organic anion transporting polypeptide 4 (Oatp4) in rat liver and comparison of its substrate specificity with Oatp1, Oatp2 and Oatp3. *Pflügers Arch* 443: 188–195, 2001.
- Eckhardt U, Schroeder A, Stieger B, Hochli M, Landmann L, Tynes R, Meier PJ, Hagenbuch B. Polyspecific substrate uptake by the hepatic organic anion transporter Oatp1 in stably transfected CHO cells. *Am J Physiol Gastrointest Liver Physiol* 276: G1037–G1042, 1999.
- Fei YJ, Liu W, Prasad PD, Kekuda R, Oblak TG, Ganapathy V, Leibach FH. Identification of the histidyl residue obligatory for the catalytic activity of the human H^+ /peptide cotransporters PEPT1 and PEPT2. *Biochemistry* 36: 452–460, 1997.
- Fujiwara K, Adachi H, Nishio T, Unno M, Tokui T, Okabe M, Onogawa T, Suzuki T, Asano N, Tanemoto M, Seki M, Shiiba K, Suzuki M, Kondo Y, Nunoki K, Shimosegawa T, Iinuma K, Ito S, Matsuno S, Abe T. Identification of thyroid hormone transporters in humans: different molecules are involved in a tissue-specific manner. *Endocrinology* 142: 2005–2012, 2001.
- Ganapathy V, Balkovetz DF, Ganapathy ME, Mahesh VB, Devoe LD, Leibach FH. Evidence for histidyl and carboxy groups at the active site of the human placental Na^+ - H^+ exchanger. *Biochem J* 245: 473–477, 1987.
- Gao B, Hagenbuch B, Kullak-Ublick GA, Benke D, Aguzzi A, Meier PJ. Organic anion-transporting polypeptides mediate transport of opioid peptides across blood-brain barrier. *J Pharmacol Exp Ther* 294: 73–79, 2000.
- Gao B, Stieger B, Noe B, Fritschy JM, Meier PJ. Localization of the organic anion transporting polypeptide 2 (Oatp2) in capillary endothelium and choroid plexus epithelium of rat brain. *J Histochem Cytochem* 47: 1255–1264, 1999.
- Grillo FG, Aronson PS. Inactivation of the renal microvillus membrane Na^+ - H^+ exchanger by histidine-specific reagents. *J Biol Chem* 261: 1120–1125, 1986.
- Gui C, Miao Y, Thompson L, Wahlgren B, Mock M, Stieger B, Hagenbuch B. Effect of pregnane X receptor ligands on transport mediated by human OATP1B1 and OATP1B3. *Eur J Pharmacol* 584: 57–65, 2008.
- Hagenbuch B, Meier PJ. Organic anion transporting polypeptides of the OATP/SLC21 family: Phylogenetic classification as OATP/SLCO superfamily, new nomenclature and molecular/functional properties. *Pflügers Arch* 447: 653–665, 2004.
- Hagenbuch B, Scharschmidt BF, Meier PJ. Effect of antisense oligonucleotides on the expression of hepatocellular bile acid and organic anion uptake systems in *Xenopus laevis* oocytes. *Biochem J* 316: 901–904, 1996.
- Hori R, Maegawa H, Kato M, Katsura T, Inui K. Inhibitory effect of diethyl pyrocarbonate on the H^+ /organic cation antiport system in rat renal brush-border membranes. *J Biol Chem* 264: 12232–12237, 1989.
- Huber RD, Gao B, Sidler Pfandler MA, Zhang-Fu W, Leuthold S, Hagenbuch B, Folkers G, Meier PJ, Stieger B. Characterization of two splice variants of human organic anion transporting polypeptide 3A1 isolated from human brain. *Am J Physiol Cell Physiol* 292: C795–C806, 2007.
- Ichikawa M, Kato Y, Miyauchi S, Sawada Y, Iga T, Fuwa T, Hanano M, Sugiyama Y. Effect of perfusate pH on the influx of 5'- ^{3}H -dimethyl-oxazolidine-2,4-dione and dissociation of epidermal growth factor from the cell-surface receptor: the existence of the proton diffusion barrier in the Disse space. *J Hepatol* 20: 190–200, 1994.
- Jacquemin E, Hagenbuch B, Stieger B, Wolkoff AW, Meier PJ. Expression cloning of a rat liver Na^+ -independent organic anion transporter. *Proc Natl Acad Sci USA* 91: 133–137, 1994.
- Kanai N, Lu R, Bao Y, Wolkoff AW, Schuster VL. Transient expression of oatp organic anion transporter in mammalian cells: identification of candidate substrates. *Am J Physiol Renal Physiol* 270: F319–F325, 1996.
- Kato M, Maegawa H, Okano T, Inui K, Hori R. Effect of various chemical modifiers on H^+ coupled transport of cephadrine via dipeptide carriers in rabbit intestinal brush-border membranes: role of histidine residues. *J Pharmacol Exp Ther* 251: 745–749, 1989.
- Kleyman TR, Cragoe EJ Jr. Amiloride and its analogs as tools in the study of ion transport. *J Membr Biol* 105: 1–21, 1988.
- Kobayashi D, Nozawa T, Imai K, Nezu J, Tsuji A, Tamai I. Involvement of human organic anion transporting polypeptide OATP-B (SLC21A9) in pH-dependent transport across intestinal apical membrane. *J Pharmacol Exp Ther* 306: 703–708, 2003.
- König J, Cui Y, Nies AT, Keppler D. Localization and genomic organization of a new hepatocellular organic anion transporting polypeptide. *J Biol Chem* 275: 23161–23168, 2000.
- König J, Cui Y, Nies AT, Keppler D. A novel human organic anion transporting polypeptide localized to the basolateral hepatocyte membrane. *Am J Physiol Gastrointest Liver Physiol* 278: G156–G164, 2000.
- König J, Seithel A, Gradhand U, Fromm MF. Pharmacogenomics of human OATP transporters. *Naunyn-Schmiedeberg's Arch Pharmacol* 372: 432–443, 2006.
- Kottra G, Daniel H. Bidirectional electrogenic transport of peptides by the proton-coupled carrier PEPT1 in *Xenopus laevis* oocytes: its asymmetry and symmetry. *J Physiol* 536: 495–503, 2001.
- Kozak M. At least six nucleotides preceding the AUG initiator codon enhance translation in mammalian cells. *J Mol Biol* 196: 947–950, 1987.
- Kramer W, Girbig F, Petzoldt E, Leipe I. Inactivation of the intestinal uptake system for beta-lactam antibiotics by diethylpyrocarbonate. *Biochim Biophys Acta* 943: 288–296, 1988.
- Kullak-Ublick GA, Hagenbuch B, Stieger B, Schteingart CD, Hofmann AF, Wolkoff AW, Meier PJ. Molecular and functional character-

- ization of an organic anion transporting polypeptide cloned from human liver. *Gastroenterology* 109: 1274–1282, 1995.
31. Kullak-Ublick GA, Ismail MG, Stieger B, Landmann L, Huber R, Pizzagalli F, Fattinger K, Meier PJ, Hagenbuch B. Organic anion-transporting polypeptide B (OATP-B) and its functional comparison with three other OATPs of human liver. *Gastroenterology* 120: 525–533, 2001.
 32. Li L, Lee TK, Meier PJ, Ballatori N. Identification of glutathione as a driving force and leukotriene C₄ as a substrate for oatp1, the hepatic sinusoidal organic solute transporter. *J Biol Chem* 273: 16184–16191, 1998.
 33. Li L, Meier PJ, Ballatori N. Oatp2 mediates bidirectional organic solute transport: a role for intracellular glutathione. *Mol Pharmacol* 58: 335–340, 2000.
 34. Marin JJ, Mangas D, Martinez-Diez MC, El-Mir MY, Briz O, Serrano MA. Sensitivity of bile acid transport by organic anion-transporting polypeptides to intracellular pH. *Biochim Biophys Acta* 1611: 249–257, 2003.
 35. Meier-Abt F, Faulstich H, Hagenbuch B. Identification of phalloidin uptake systems of rat and human liver. *Biochim Biophys Acta* 1664: 64–69, 2004.
 36. Meier-Abt F, Mokrab Y, Mizuguchi K. Organic anion transporting polypeptides of the OATP/SLCO superfamily: identification of new members in nonmammalian species, comparative modeling and a potential transport mode. *J Membr Biol* 208: 213–227, 2005.
 37. Mikkaichi T, Suzuki T, Onogawa T, Tanemoto M, Mizutamari H, Okada M, Chaki T, Masuda S, Tokui T, Eto N, Abe M, Satoh F, Unno M, Hishinuma T, Inui K, Ito S, Goto J, Abe T. Isolation and characterization of a digoxin transporter and its rat homologue expressed in the kidney. *Proc Natl Acad Sci USA* 101: 3569–3574, 2004.
 38. Miles EW. Modification of histidyl residues in proteins by diethylpyrocarbonate. *Methods Enzymol* 47: 431–442, 1977.
 39. Nishimura T, Kubo Y, Kato Y, Sai Y, Ogihara T, Tsuji A. Characterization of the uptake mechanism for a novel loop diuretic, M17055, in Caco-2 cells: involvement of organic anion transporting polypeptide (OATP)-B. *Pharm Res* 24: 90–98, 2007.
 40. Noe B, Hagenbuch B, Stieger B, Meier PJ. Isolation of a multispecific organic anion and cardiac glycoside transporter from rat brain. *Proc Natl Acad Sci USA* 94: 10346–10350, 1997.
 41. Noe J, Portmann R, Brun ME, Funk C. Substrate-dependent drug-drug interactions between gemfibrozil, fluvastatin and other organic anion-transporting peptide (OATP) substrates on OATP1B1, OATP2B1, and OATP1B3. *Drug Metab Dispos* 35: 1308–1314, 2007.
 42. Nozawa T, Imai K, Nezu J, Tsuji A, Tamai I. Functional characterization of pH-sensitive organic anion transporting polypeptide OATP-B in human. *J Pharmacol Exp Ther* 308: 438–445, 2004.
 43. Palermo DP, DeGraaf ME, Marotti KR, Rehberg E, Post LE. Production of analytical quantities of recombinant proteins in Chinese hamster ovary cells using sodium butyrate to elevate gene expression. *J Biotechnol* 19: 35–47, 1991.
 44. Pizzagalli F, Hagenbuch B, Stieger B, Klenk U, Folkers G, Meier PJ. Identification of a novel human organic anion transporting polypeptide as a high affinity thyroxine transporter. *Mol Endocrinol* 16: 2283–2296, 2002.
 45. Pizzagalli F, Varga Z, Huber RD, Folkers G, Meier PJ, and St-Pierre MV. Identification of steroid sulfate transport processes in the human mammary gland. *J Clin Endocrinol Metab* 88: 3902–3912, 2003.
 46. Pushkin A, Kurtz I. SLC4 base (HCO₃⁻, CO₃²⁻) transporters: classification, function, structure, genetic diseases, and knockout models. *Am J Physiol Renal Physiol* 290: F580–F599, 2006.
 47. Reichel C, Gao B, Van Montfort J, Cattori V, Rahner C, Hagenbuch B, Stieger B, Kamisako T, Meier PJ. Localization and function of the organic anion-transporting polypeptide Oatp2 in rat liver. *Gastroenterology* 117: 688–695, 1999.
 48. Rink TJ, Tsien RY, Pozzan T. Cytoplasmic pH and free Mg²⁺ in lymphocytes. *J Cell Biol* 95: 189–196, 1982.
 49. Romero MF, Fulton CM, Boron WF. The SLC4 family of HCO₃⁻ transporters. *Pflügers Arch* 447: 495–509, 2004.
 50. Roos A, and Boron WF. Intracellular pH. *Physiol Rev* 61: 296–434, 1981.
 51. Rotin D, Grinstein S. Impaired cell volume regulation in Na⁺-H⁺ exchange-deficient mutants. *Am J Physiol Cell Physiol* 257: C1158–C1165, 1989.
 52. Sai Y, Kaneko Y, Ito S, Mitsuoka K, Kato Y, Tamai I, Artursson P, Tsuji A. Predominant contribution of organic anion transporting polypeptide OATP-B (OATP2B1) to apical uptake of estrone-3-sulfate by human intestinal Caco-2 cells. *Drug Metab Dispos* 34: 1423–1431, 2006.
 53. Said HM, Mohammadkhani R. Folate transport in intestinal brush border membrane: involvement of essential histidine residue(s). *Biochem J* 290: 237–240, 1993.
 54. Satlin LM, Amin V, Wolkoff AW. Organic anion transporting polypeptide mediates organic anion/HCO₃⁻ exchange. *J Biol Chem* 272: 26340–26345, 1997.
 55. Schroeder A, Eckhardt U, Stieger B, Tynes R, Schteingart CD, Hofmann AF, Meier PJ, Hagenbuch B. Substrate specificity of the rat liver Na⁺-bile salt cotransporter in *Xenopus laevis* oocytes and in CHO cells. *Am J Physiol Gastrointest Liver Physiol* 274: G370–G375, 1998.
 56. Smith PK, Krohn RI, Hermanson GT, Mallia AK, Gartner FH, Provenzano MD, Fujimoto EK, Goeke NM, Olson BJ, Klenk DC. Measurement of protein using bicinchoninic acid. *Anal Biochem* 150: 76–85, 1985.
 57. Tamai I, Nezu J, Uchino H, Sai Y, Oku A, Shimane M, Tsuji A. Molecular identification and characterization of novel members of the human organic anion transporter (OATP) family. *Biochem Biophys Res Commun* 273: 251–260, 2000.
 58. Thomas RC. The effect of carbon dioxide on the intracellular pH and buffering power of snail neurones. *J Physiol* 255: 715–735, 1976.
 59. Thwaites DT, Anderson CM. H⁺-coupled nutrient, micronutrient and drug transporters in the mammalian small intestine. *Exp Physiol* 92: 603–619, 2007.
 60. Treiber A, Schneider R, Hausler S, Stieger B. Bosentan is a substrate of human OATP1B1 and OATP1B3: inhibition of hepatic uptake as the common mechanism of its interactions with cyclosporin A, rifampicin, and sildenafil. *Drug Metab Dispos* 35: 1400–1407, 2007.
 61. Tsuji A, Terasaki T, Tamai I, Hirooka H. H⁺ gradient-dependent and carrier-mediated transport of cefixime, a new cephalosporin antibiotic, across brush-border membrane vesicles from rat small intestine. *J Pharmacol Exp Ther* 241: 594–601, 1987.
 62. Walters HC, Craddock AL, Fusegawa H, Willingham MC, Dawson PA. Expression, transport properties, and chromosomal location of organic anion transporter subtype 3. *Am J Physiol Gastrointest Liver Physiol* 279: G1188–G1200, 2000.
 63. Wang D, Balkovetz DF, Warnock DG. Mutational analysis of transmembrane histidines in the amiloride-sensitive Na⁺/H⁺ exchanger. *Am J Physiol Cell Physiol* 269: C392–C402, 1995.
 64. Winter C, Schulz N, Giebisch G, Geibel JP, Wagner CA. Nongenomic stimulation of vacuolar H⁺-ATPases in intercalated renal tubule cells by aldosterone. *Proc Natl Acad Sci USA* 101: 2636–2641, 2004.
 65. Zair ZM, Eloranta JJ, Stieger B, and Kullak-Ublick GA. Pharmacogenetics of OATP (SLC21/SLCO), OAT and OCT (SLC22) and PEPT (SLC15) transporters in the intestine, liver and kidney. *Pharmacogenomics* 9: 597–624, 2008.